

Electronic Supporting Information

Copper nanoclusters-Ru(dcbpy)₃²⁺ as a cathodic ECL-RET probe combined 3D bipedal DNA walker amplification for bioanalysis

Xumei Zhou¹, Mingjing Li¹, Shengfang Niu, Jing Han*, Sanping Chen, Gang

Xie*

*Key Laboratory of Synthetic and Natural Functional Molecule of the Ministry of Education,
College of Chemistry & Materials Science, Northwest University, Xi'an, Shaanxi 710127, P. R.
China*

¹ These authors contributed equally to this work.

*** Corresponding author: Jing Han and Gang Xie**

E-mail: hanjing@nwu.edu.cn, xiegang@nwu.edu.cn.

Table of Contents

| | |
|--|-----|
| 1. Experimental section | S3 |
| 1.1. Reagent and materials | S3 |
| 1.2. Apparatus | S4 |
| 1.3. ECL measurements and characterization parameters | S4 |
| 2. ECL mechanism | S5 |
| 3. Relative ECL Efficiency of Cu NCs-Ru | S6 |
| 4. The ECL spectra of Cu NCs, Ru(dcbpy) ₃ ²⁺ and Cu NCs-Ru | S8 |
| 5. Optimization of experimental conditions | S9 |
| 6. Comparison with other works for PDGF-BB detection | S11 |
| 7. Recovery assay of PDGF-BB in human serum samples | S11 |
| 8. Selectivity of PDGF-BB in human serum samples | S12 |

1. Experimental section

1.1. Reagents and materials

Tris (4,4'-dicarboxylic acid-2,2'-bipyridyl) ruthenium (II) dichloride ($\text{Ru}(\text{dcbpy})_3^{2+}$) was obtained from Suna Tech Inc. (Suzhou, China). *L*-ascorbic acid (*L*-AA), copper sulfate (CuSO_4), *N*-(3-dimethylaminopropyl)-*N'*-ethylcarbodiimide hydrochloride (EDC) and *N*-Hydroxy succinimide (NHS) were supplied by Sigma-Aldrich Chemical Co. (St. Louis, USA). Carboxyl-modified magnetic nanoparticles (MNPs) were obtained from BaseLine ChromTech Research Centre (Tianjin, China). Potassium peroxodisulfate ($\text{K}_2\text{S}_2\text{O}_8$) was received from Aladdin Ltd. (Shanghai, China). Nb.BbvCI enzyme and 10×CutSmart buffer were bought from New England Biolabs Inc. (USA). NaOH, bovine serum albumin (BSA) and hemoglobin (Hb) were purchased from J&K Scientific Ltd. (Beijing, China). Insulin was provided by Shanghai LincBio Science Co. Ltd. All oligonucleotides were synthesized and purified by Sangon Biological Engineering Technology and Services Co., Ltd. (Shanghai, China). Each oligonucleotide was heated to 95 °C for 5 min and cooled naturally before use. Sequence information of the DNA was listed in Table S1.

Table S1. Sequence of the oligonucleotides employed in this work

| Name | Sequences (5'-3') |
|--------|---|
| HP1 | 5'-  CAGGCTACGGCACGTAGAGCATCACCATGATCCTG(T) ₁₅ CGACATCTAACG TCCTCAGCCAGGATCA-3' |
| Fc-HP2 | 5'-NH ₂ -TTTGT  TGATCCTGGC*TGAGGAGCAATAGGATCAAC-Fc-3' |

Where '*' was the cleavage site of Nb.BbvCI and the same color label was paired DNA sequence.

1.2. Apparatus

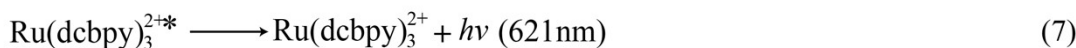
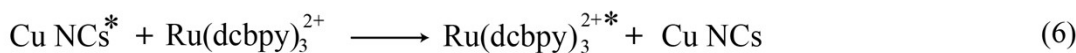
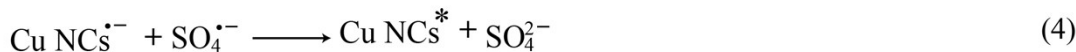
ECL measurements were carried out with an MPI-E electrochemiluminescence analytical system (Xi'an Remax analyse instrument Co. Ltd, China). CV test was executed on a CHI660E electrochemical workstation (Shanghai CH Instruments, Co., China). All experiments adopted a conventional three-electrode system with the modified glassy carbon electrode (GCE, $\Phi = 3$ mm) as working electrode, an Ag/AgCl (saturated KCl) electrode as reference electrode and a platinum wire as auxiliary electrode, respectively. Transmission electron microscope (TEM, Thermo Fisher, USA), fluorescence spectrophotometer (FL, Hitachi F-4500, Japan) and X-ray photoelectron spectra (XPS, ULVAC-PHI, Japan) were used for morphology, elemental composition and structure characterization.

1.3. ECL measurements and characterization parameters

For the ECL detection, the prepared aptasensor was inserted into 3 mL of 0.1 M S₂O₈²⁻ (PBS, pH 7.4) and experimental data was collected using MPI-E ECL analytical system. The parameters were involved of -1.7 to 0 V potential range, 0.1 V s⁻¹ scan rate and PMT high-voltage 800 V. And the ECL intensity peak values were employed for the quantitative analysis. The modification of each steps were characterized by CV in 5 mM Fe(CN)₆^{4-/3-} and the parameters were included of -0.2 to 0.6 V potential range and 0.1 V s⁻¹ scan rate.

2. ECL mechanism

According to the researchers previously established mechanisms,^{1,2} the integrated ECL-RET process could be described by the following steps: First, Cu NCs was directly reduced to Cu NCs⁻ on the electrode (eq 1). Then, S₂O₈²⁻ was reduced to output massive amounts of S₂O₈^{3*-} (eq 2). Subsequently, S₂O₈^{3*-} was transform to SO₄⁻ (eq 3), which quickly reacted with Cu NCs⁻ to obtain excited state Cu NCs* (eq 4). Afterwards, with the unstable and excited-state Cu NCs* return to the stable and ground state Cu NCs, a ECL emission at 445 nm is produced (eq 5). As the donor of the ECL-RET system, Cu NCs* can transfer energy to Ru(dcbpy)₃²⁺ to form Ru(dcbpy)₃^{2+*}, which emits light at 621 nm and returns to the ground state (eq 6-7). Thus, the ECL signal of Cu NCs decreases, while the ECL response of Ru(dcbpy)₃²⁺ increases. The ECL-RET can be expressed as follows:



3. Relative ECL Efficiency of Cu NCs-Ru

To evaluate ECL performance of as-synthesized Cu NCs-Ru, ECL efficiency of Cu NCs-Ru relative to that of the Ru(dcbpy)₃²⁺ was measured in PBS containing 0.1 M S₂O₈²⁻. The relative ECL efficiency of as-prepared Cu NCs-Ru could be calculated by comparing the relative value of the integrated ECL intensity of Cu NCs-Ru in reference to that of Ru(dcbpy)₃²⁺ as the following equation.³

$$Q = \frac{\Phi_x}{\Phi_0} = \left(\frac{\int_0^t Idt}{\int_0^t idt} \right)_x \bigg/ \left(\frac{\int_0^t Idt}{\int_0^t idt} \right)_0$$

Here, Φ_x is the ECL efficiency of Cu NCs-Ru, Φ_0 is the ECL quantum efficiency of Ru(dcbpy)₃²⁺. “*I*” and “*i*” represent ECL intensity, and current value, respectively.

According to above equation, the relative ECL efficiency of as-synthesized Cu NCs-Ru is calculated to be ~5.196 times stronger than that of Ru(dcbpy)₃²⁺, which demonstrates that the Cu NCs can remarkably improve the ECL efficiency.

To further verify the highly efficiency of intramolecular ECL-RET, ECL measurements of product of Cu NCs-Ru and the simple mixture of Cu NCs with Ru(dcbpy)₃²⁺ in 0.1 M S₂O₈²⁻ were measured. According to Fig. S1A, it can be observed that the Cu NCs-Ru (curve a) shows a stronger ECL intensity than the simple mixture of Cu NCs with Ru(dcbpy)₃²⁺ (curve b), owing to intramolecular

ECL-RET can efficiently decrease electron transfer distance and further enhancing ECL efficiency. In addition, it can be seen from Fig. S1B, the ECL peak of Cu NCs-Ru appears 0.1 s faster than the individual Cu NCs mixed with Ru(dcbpy)₃²⁺. The above results manifest that intramolecular ECL-RET of Cu NCs-Ru can improve ECL efficiency of Ru(dcbpy)₃²⁺ on account of significantly decrease the energy loss.

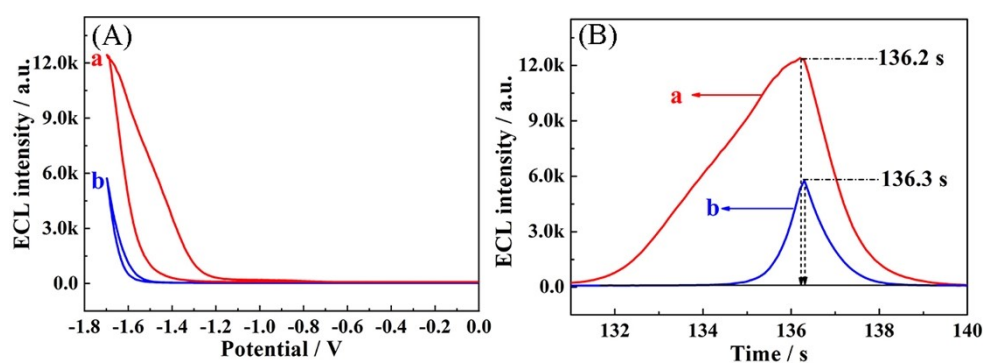


Fig. S1. (A) ECL-potential curves and (B) ECL-time curves of (a) Cu NCs-Ru(dcbpy)₃²⁺ composite and (b) simple mixture of Cu NCs with Ru(dcbpy)₃²⁺.

4. The ECL spectra of Cu NCs, Ru(dcbpy)₃²⁺ and Cu NCs-Ru

The ECL spectra of Cu NCs, Ru(dcbpy)₃²⁺ and Cu NCs-Ru were measured in 0.1 M S₂O₈²⁻ (PBS, pH=7.4) with a sequence of optical filters. As shown in the following Fig. S2, the ECL emission peak of Cu NCs appeared at around 445 nm (curve a) and the ECL spectrum peak corresponding to Ru(dcbpy)₃²⁺ was located at around 621 nm (curve b). When the composite of Cu NCs-Ru was modified on GCE, there existed dual ECL emission peak. Meanwhile, the ECL emission peak at 445 nm decreased while the ECL emission peak at 621 nm increased (curve c). The above results demonstrated that the highly efficient ECL-RET in one nanostructure between Cu NCs and Ru(dcbpy)₃²⁺.

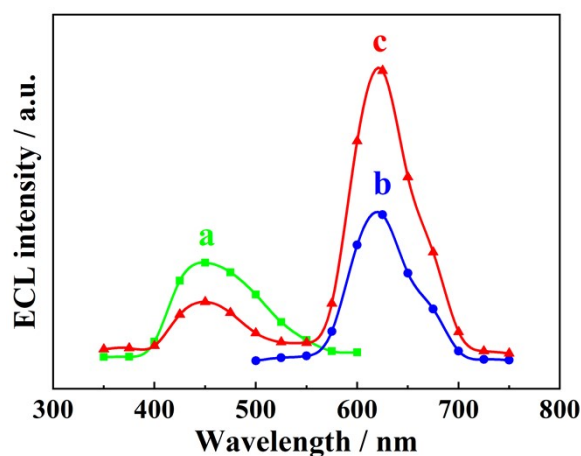


Fig. S2. ECL spectra of (a) Cu NCs, (b) Ru(dcbpy)₃²⁺ and (c) Cu NCs-Ru composite were performed in 0.1 M S₂O₈²⁻ (PBS, pH=7.4) using a sequence of filters

5. Optimization of experimental conditions

In order to achieve the optimal performance and further practical application of the fabricated aptasensor platform, the proportion of $\text{Ru}(\text{dcbpy})_3^{2+}$ and Cu NCs, the concentration of CP, the incubation time of Nb.BbvCI, and the concentration of Nb.BbvCI were optimized. First, the proportion of $\text{Ru}(\text{dcbpy})_3^{2+}$ and Cu NCs which was closely related to the initial signal of the aptasensor was optimized. As exhibited in Fig. S2A, as the ratio of $\text{Ru}(\text{dcbpy})_3^{2+}$ and Cu NCs changes from 1:4 to 4:1, the ECL intensity increases correspondingly and achieves a maximum at 1:1. Thus, the proportion of 1:1 is selected as the optimum proportion of $\text{Ru}(\text{dcbpy})_3^{2+}$ and Cu NCs. As displayed in Fig. S2B, it is evident that the ECL intensity decreases rapidly, with increasing concentration of CP and reaches a platform at 1.0, which is chosen as the suitable experimental parameter.⁴ As seen in Fig. S2C, when the incubation time of Nb.BbvCI increases from 0 to 2 h, the ECL response occurs very quickly decreasing and the platform can be observed at 2 h. So, 2 h is chosen as the most appropriate enzymatic cleavage reaction time in this system. As described in Fig. S2D, the concentration of Nb.BbvCI from 0 to 1.5 $\text{U } \mu\text{L}^{-1}$ keeps a decreasing ECL intensity and achieves a platform at 1.0 $\text{U } \mu\text{L}^{-1}$. Hence, 1.0 $\text{U } \mu\text{L}^{-1}$ is selected as most optimal concentration of Nb.BbvCI. Therefore, the above optimal conditions are used for further experiments.

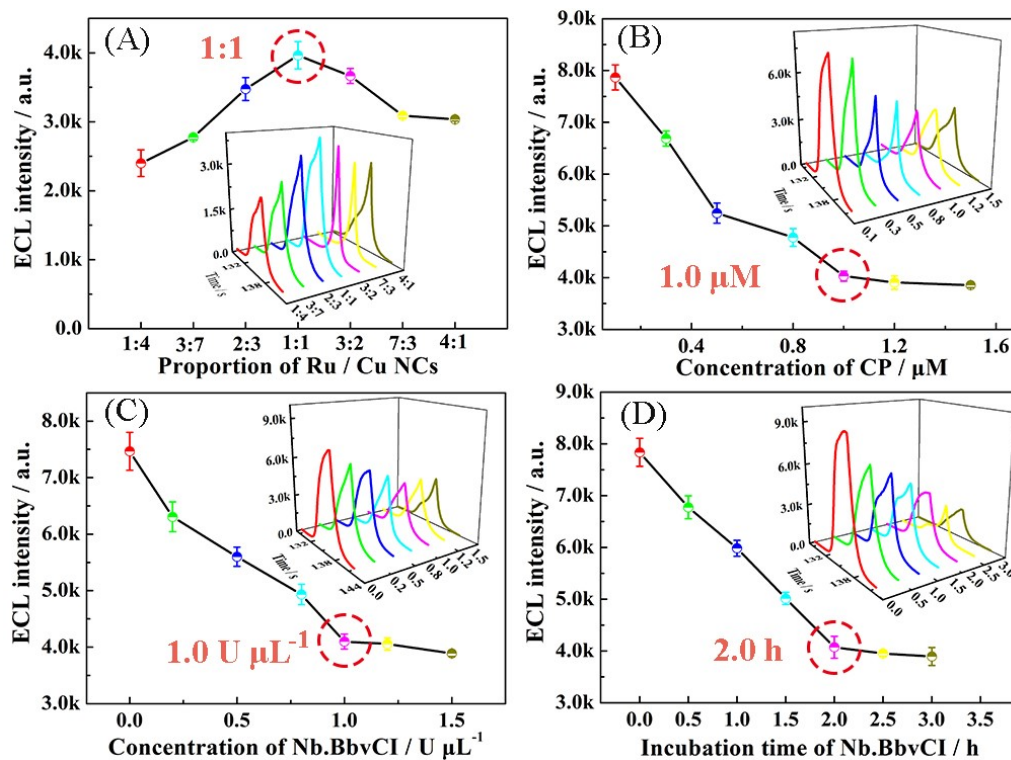


Fig. S3. Influence of (A) the proportion of $Ru(dcbpy)_3^{2+}$ and Cu NCs, (B) the concentration of CP, (C) the incubation time of Nb.BbvCI, and (D) the concentration of Nb.BbvCI for the detection of PDGF-BB (100 pM) in PBS containing 0.1 M $S_2O_8^{2-}$ (pH 7.4) under the same measurement conditions.

6. Comparison with other works for PDGF-BB detection

Table S2. Comparison with other works for PDGF-BB detection

| Detection method | Linear range | Detection limit | References |
|------------------|------------------|-----------------|------------|
| Fluorescence | 0.2 nM to 100 nM | 0.13 nM | 5 |
| Luminescence | 10 pM to 300 pM | 10 pM | 6 |
| ECL | 20 pM to 80 nM | 13 pM | 7 |
| Fluorescence | 2.5 pM to 300 pM | 826 fM | 8 |
| ELISA | 0.5 nM to 10 nM | 0.08 nM | 9 |
| ECL | 0.01 pM to 10 nM | 3.5 fM | 10 |
| ECL | 10 fM to 10 nM | 3.3 fM | This work |

Abbreviations: EC–Electrochemical detection; ECL–Electrochemiluminescence detection

7. Recovery assay of PDGF-BB in human serum samples

Table S3. Recovery assay of PDGF-BB in human serum samples

| Samples | Added (pM) | Found (pM) | Recovery (%) | RSD (%) |
|---------|------------|------------|--------------|---------|
| 1 | 0.1 | 0.092 | 92.17 | 2.12 |
| 2 | 0.5 | 0.527 | 105.40 | 3.39 |
| 3 | 5 | 5.531 | 110.63 | 3.21 |
| 4 | 100 | 103.271 | 103.27 | 4.11 |
| 5 | 1000 | 1061.503 | 106.15 | 4.77 |

8. Selectivity of PDGF-BB in human serum samples

As shown in Fig. S4, when 100-fold interferences (ascorbic acid (AA), dopamine (DPA), uric acid (UA), glucose (Glu) and Cu ions (Cu^{2+})) are employed to replace the target PDGF-BB in 100-fold diluted human serum sample, respectively, no apparent changes of ECL responses are observed compared with the other interferences in 0.1 M $\text{S}_2\text{O}_8^{2-}$ (PBS, pH=7.4). In 100-fold diluted human serum sample, the ECL response of PDGF-BB exhibits similar ECL intensities compared with in 0.1 M $\text{S}_2\text{O}_8^{2-}$ (PBS, pH=7.4). These results indicated that the developed aptasensor exhibited an acceptable specificity in the human serum sample.

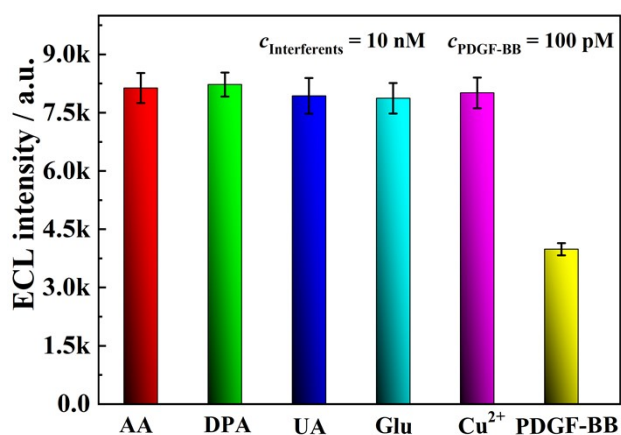


Fig. S4. Selectivity assessment for PDGF-BB detection against other interference: ascorbic acid (AA), dopamine (DPA), uric acid (UA), glucose (Glu) and Cu ions (Cu^{2+}) in 100-fold diluted human serum samples.

References

- 1 D. Ege, W. G. Becker and A. J. Bard, *Anal. Chem.*, 1984, **56**, 2413–2417.
- 2 D. Qin, S. Meng, Y. Wu, G. Mo, X. Jiang, B. Deng, *ACS Sustainable Chem. Eng.*, 2021, **9**, 7541–7549.

- 3 F. Wang, J. Lin, T. Zhao, D. Hu, T. Wu and Y. Liu, *J. Am. Chem. Soc.*, 2016, **138**, 7718–7724.
- 4 W. X. Lv, Q. T. Yang, Q. Li, H. Li and F. Li, *Anal. Chem.*, 2020, **92**, 11747–11754.
- 5 A. Bahreyni, S. Tahmasebi, M. Ramezani, M. Alibolandi, N. M. Danesh, K. Abnous and S. M. Taghdisi, *Sens. Actuators B Chem.*, 2019, **280**, 10–15.
- 6 L. Lu, Z. Mao, T. S. Kang, C. H. Leung and D. L. Ma, *Biosens. Bioelectron.*, 2016, **85**, 300–309.
- 7 H. F. Xu, S. J. Liang, X. Zhu, X. Q. Wu, Y. Q. Dong, H. S. Wu, W. X. Zhang and Y. W. Chi, *Biosens. Bioelectron.*, 2017, **92**, 695–701.
- 8 Y. B. Li, J. Shao, W. T. Guo and M. T. Wang, *Microchimica Acta*, 2019, **186**, 155–161.
- 9 S. Gao, X. X. Zheng and J. H. Wu, *Biosens. Bioelectron.*, 2018, **102**, 57–62.
- 10 Y. Y. Chang, M. Li, Z. Wu, Y. Zhuo, Y. Q. Chai, Q. Xiao and R. Yuan, *Anal. Chem.*, 2018, **90**, 8241–8247.